



# MiR-322-5p Alleviates Cell Injury and Impairment of Cognitive Function in Vascular Dementia by Targeting TSPAN5

Wei Zheng<sup>1</sup>, Jie Zhang<sup>1</sup>, Bin Zhou<sup>1</sup>, and Huanxian Chang<sup>2</sup>

<sup>1</sup>Department of Rehabilitation Medicine, The Affiliated Lianyungang Oriental Hospital of Xuzhou Medical University, Lianyungang, Jiangsu;

<sup>2</sup>Department of Neurology, The Affiliated Lianyungang Oriental Hospital of Xuzhou Medical University, Lianyungang, Jiangsu, China.

**Purpose:** As the population ages, the incidence of clinical dementia has been rising around the world. It has been reported that microRNAs act as key diagnostic biomarkers and targets for various neurological conditions, including dementia. MiR-322-5p has been revealed to play an important role in multiple diseases. In this study, we aimed to investigate the role and regulatory mechanism of miR-322-5p in vascular dementia.

**Materials and Methods:** In this study, neonatal rat neurons (NRNs) were subjected to oxygen-glucose deprivation/reoxygenation (OGD/R) to induce cell injury. The animals were subjected to permanent bilateral occlusion of the carotid arteries (2-vessel occlusion, 2VO) to induce the model of chronic brain hypoperfusion.

**Results:** MiR-322-5p expression was significantly downregulated in the neurons exposed to OGD/R and the hippocampi of 2VO rats. Overexpression of miR-322-5p ameliorated cell apoptosis and the inflammatory response in vitro. In a mechanistic study, miR-322-5p was confirmed to directly target and negatively regulate tetraspanin 5 (TSPAN5) in cultured NRNs. Moreover, overexpression of TSPAN5 could counteract the effects of miR-322-5p overexpression on cell apoptosis and the inflammatory response in OGD/R-treated neurons. More importantly, miR-322-5p improved cognitive ability and inhibited inflammatory production in 2VO rats.

**Conclusion:** Overall, the results suggest that miR-322-5p alleviates vascular dementia development by targeting TSPAN5. This discovery may provide a potential therapeutic target for dementia.

**Key Words:** Vascular dementia, miR-322-5p, TSPAN5

## INTRODUCTION

Chronic brain hypoperfusion (CBH) is a typical clinical feature of vascular dementia or Alzheimer's disease that can result in learning and memory impairments.<sup>1,2</sup> CBH has been found to affect various biological processes, such as by induc-

ing autophagic-lysosomal neuropathology, glial activation, inflammatory response, a decline in dendritic spine density, and white matter impairment.<sup>3</sup> However, the molecular regulatory mechanisms underlying vascular dementia development are not fully understood. Therefore, it is critical to find effective molecular targets for vascular dementia.

MicroRNAs (miRNAs) are a class of short endogenous transcripts (18-24 nts) without protein-coding ability.<sup>4,5</sup> It has been widely documented that miRNAs can bind the 3'-untranslated regions (3'-UTRs) of messenger RNAs (mRNAs) to affect the progression of various central nervous system diseases. For example, miR-let-7a targets signal transducer and activator of transcription 3 to repress the  $\alpha$ -synuclein-induced microglial inflammation in Parkinson's disease.<sup>6</sup> Moreover, miR-27a was reported to exert effects on cerebral cavernous malformations by targeting VE-cadherin in mice.<sup>7</sup> Several miRNAs play important roles in neurodegenerative diseases.<sup>8,9</sup> MiR-219-5p sponges

**Received:** August 13, 2021 **Revised:** November 12, 2021

**Accepted:** November 16, 2021

**Corresponding author:** Jie Zhang, MM, Department of Rehabilitation Medicine, The Affiliated Lianyungang Oriental Hospital of Xuzhou Medical University, 57 Zhonghua West Road, Lianyungang District, Lianyungang 222042, Jiangsu, China.  
Tel: 86-18260388116, Fax: 86-0518-82309111, E-mail: zhangjie08@hotmail.com

•The authors have no potential conflicts of interest to disclose.

© Copyright: Yonsei University College of Medicine 2022

This is an Open Access article distributed under the terms of the Creative Commons Attribution Non-Commercial License (<https://creativecommons.org/licenses/by-nc/4.0>) which permits unrestricted non-commercial use, distribution, and reproduction in any medium, provided the original work is properly cited.

tau-tubulin kinase1 and glycogen synthase kinase-3 $\beta$  to inhibit tau phosphorylation in Alzheimer's disease.<sup>10</sup> MiR-361-3p targets  $\beta$ -amyloid-precursor-protein-cleaver-enzyme 1 to decrease  $\beta$ -amyloid accumulation and alleviate cognitive deficits in Alzheimer's disease.<sup>11</sup> MiR-195 has an anti-amyloidogenic effect to protect against dementia caused by CBH in rats.<sup>12</sup> MiR-9 was identified to regulate CBH-induced dementia by targeting  $\beta$ -amyloid-precursor-protein-cleaver-enzyme 1.<sup>13</sup> The role of miR-322-5p, previously known as miR-322, has been investigated in multiple biological processes. MiR-322-5p has a downregulated expression in the hearts of rats with pulmonary hypertension.<sup>14</sup> MiR-322 stabilizes mRNA to dampen the extracellular signal-regulated kinase 1/2 phosphorylation in cartilage.<sup>15</sup> Importantly, miR-322-5p was found to be related to degradation of brain-derived neurotrophic factor (BDNF), a decrease in the level of which is a pathophysiological hallmark in the brain in Alzheimer's disease.<sup>16</sup> However, there has been no study that focused on the role of miR-322-5p in vascular dementia.

The present study aimed to explore the role and regulatory mechanism of miR-322-5p in vascular dementia. We found that miR-322-5p alleviated CHB-induced vascular dementia by targeting tetraspanin 5 (TSPAN5). MiR-322-5p was investigated in the context of vascular dementia for the first time, and the findings may provide a potential therapeutic target for vascular dementia.

## MATERIALS AND METHODS

### Animals and grouping

A total of 40 Sprague-Dawley rats (male, 220–260 g, 8 weeks old) were purchased from Vital River Co., Ltd. (Beijing, China). All animals were housed at 23 $\pm$ 1°C and 55 $\pm$ 5% humidity and maintained on a 12-h dark-light artificial cycle with free access to food and water. All animal experiments were carried out in strict accordance with the recommendations in the Guide for the Care and Use of Laboratory Animals of the National Institutes of Health and were approved by the Institutional Animal Care and Use Committee of the Affiliated Lianyungang Oriental Hospital of Xuzhou Medical University (Jiangsu, China) (approval no. 2018-021).

### Bilateral occlusion of carotid artery (2-vessel occlusion) surgery

2-vessel occlusion (2VO) was induced in rats as described previously.<sup>12,17</sup> The rats were anaesthetized with intraperitoneal injection of ketamine (40 mg/kg) and xylazine (10 mg/kg; Sigma-Aldrich, St Louis, MO, USA). Then, the rats were placed on an electric heating pad, and their body temperature was maintained at 37°C. The fur around the neck was shaved off with an electric shaver, and the skin was sterilized with 75% alcohol. Both common carotid arteries were exposed through a 1.5–2 cm midline cervical incision. The vagus nerves were careful-

ly separated, and both common carotid arteries were permanently ligated with 5–0 silk sutures (Jinhuan Medical, Ltd., Shanghai, China). The sham-operated animals were treated similarly to the 2VO rats, but the common carotid artery was not ligated. After the wounds were sutured, the rats were allowed to recover from anesthesia before being returned to their cages. None of the rats died during the experiment. The tests were terminated when the rats had lost >15% of their body weight (body weight prior to injection).

Before the operation, the rats were randomly divided into four equal groups (n=8 per group). A total of four groups were used in our experiments: sham group (underwent 2VO surgery without ligation); 2VO group (underwent 2VO surgery with ligation); 2VO+LV-NC (lentiviral vector-negative control) group (underwent 2VO surgery and received injection of empty LV); and 2VO+LV-miR-322-5p group (underwent 2VO surgery and received injection of LV-miR-322-5p).

### Construction of miR-322-5p lentiviral vectors

The purchased coding oligonucleotides of antisense rat miR-322-5p mimics (Guangzhou RiboBio Co., Ltd., Guangzhou, China) were cloned and inserted into a lentivirus expression vector, pCDH1-MCS1-EF1-copGFP (LV-miR-322-5p) (System Biosciences, Inc., Mountain View, CA, USA). An empty lentiviral vector (LV-NC) acted as a control. The short hairpin RNA of TSPAN5 was synthesized and cloned into the lentiviral expression vector piLenti-siRNA-GFP (LV-sh-TSPAN5) (Applied Biological Materials Inc., Richmond, Canada). The concentrated virus stocks were titered in 5 $\times$ 10<sup>4</sup> cells/mL HEK293T cells at 37°C for 72 h based on green fluorescent protein (GFP) expression. Lentiviral vectors contained a sequence encoding GFP. Transduction efficiency was examined by fluorescence microscopy (magnification,  $\times$ 100).

### Lentiviral vector injection

One week after 2VO surgery, the rats were anesthetized and placed in a stereotaxic frame (RWB Life Science Co., Ltd., Shenzhen, China). Two microliters (1 $\times$ 10<sup>5</sup> TU/ $\mu$ L) of lentiviral vector, i.e., LV-NC, LV-miR-322-5p, or LV-TSPAN5 was injected bilaterally into the CA1 region of the rat hippocampus using a 5- $\mu$ L Hamilton syringe with a 33-gauge tip needle (Hamilton, Bonaduz, Switzerland) at a rate of 30 nL/min after a small injection hole was drilled. After the wounds were sutured, the rats were allowed to recover from anesthesia before being returned to their cages. Subsequent experiments were performed 8 weeks after injection. Samples were obtained from the hippocampus after the rats were euthanized by decapitation under carbon dioxide (CO<sub>2</sub>) anesthesia.

### Isolation of primary hippocampal neonatal rat neurons

On the first day after birth, hippocampal tissues from rat pups were collected, placed in phosphate-buffered saline (PBS; Sigma-Aldrich) on ice, and chopped. The tissues were sliced into

pieces and then incubated with trypsin (0.125%; Gibco, Thermo Fisher Scientific, Inc., Waltham, MA, USA). Subsequently, the cells were placed in poly-D-lysine-coated 6-well plates (10 µg/mL; cat. no. P7280; Sigma-Aldrich). Neonatal rat neurons (NRNs) were maintained in neurobasal medium A (Gibco, Thermo Fisher Scientific, Inc.) containing 10% fetal bovine serum (FBS; cat. no. SH30070.03; HyClone, Logan, UT, USA) and 2% B27 supplement (cat. no. 17504-044; Invitrogen, Carlsbad, CA, USA). Three days later, cytosine arabinoside (5 µmol/L; cat. no. F3504; Sigma-Aldrich) was added to the neurobasal medium to repress astrocyte proliferation. The neurons were used 10–14 days after plating for further experiments.

### Cell treatment

An NRN oxygen-glucose deprivation/reoxygenation (OGD/R) model was established according to reported procedures.<sup>18</sup> Briefly, NRNs were treated with Na<sub>2</sub>S<sub>2</sub>O<sub>4</sub> (1 mmol/L; Sigma-Aldrich) for 10 min. After being washed with PBS (Sigma-Aldrich), the NRNs were maintained in low-glucose Dulbecco's modified Eagle's medium (Gibco, Thermo Fisher Scientific, Inc.) for 3 h. NRNs in the control group were incubated under normal conditions.

### Cell transfection

MiR-322-5p mimics and NC mimics were synthesized by GenePharma (Shanghai, China). Full-length TSPAN5 was inserted into the pcDNA3.1 vector (Invitrogen) to generate a TSPAN5 overexpression vector (TSPAN5), and an empty pcDNA3.1 vector was used as a NC. Cell transfection was performed using Lipofectamine 2000 (Invitrogen).

### 3-(4,5-Dimethylthiazol-2-yl)-2,5-diphenyltetrazolium bromide (MTT) assay

The MTT kit (cat. no. M-0283; Sigma-Aldrich) was used to detect neuron viability. A total of 1×10<sup>5</sup> NRNs were seeded in a 96-well plate and transfected with the indicated vectors for 48 h. Then, 20-µL MTT solution was added to each well for 4 h of incubation, and the formazan crystals were dissolved in 150-µL dimethylsulfoxide (cat. no. D2650; Sigma-Aldrich). The absorbance was measured using a microplate reader (Molecular Devices, Sunnyvale, CA, USA) at a wavelength of 490 nm.

### Reverse transcription-quantitative PCR

Total RNA was extracted from NRNs or brain tissues using the TRIzol reagent (cat. no. 15596026; Invitrogen). The PrimeScript RT reagent kit (cat. no. HRR037A; Takara, Dalian, China) was used to transcribe RNAs into cDNAs. PCR was performed by using the SYBR Green PCR kit (cat. no. RR086A; TaKaRa) on an Applied Biosystems 7500 instrument (Thermo Fisher Scientific, Inc.). GAPDH/U6 were used as internal references. Relative expression of genes was determined using the 2<sup>-ΔΔCt</sup> method. The primer sequences used for PCR are as follows: miR-322-5p forward, 5'-CAGCAGCAATTCATGTTTTGG-3', and reverse,

5'-CTCTACAGCTATATTGCCAGCCAC-3'; TSPAN5 forward, 5'-AGGAATACTGGCAGTGCTG-3', and reverse, 5'-CTTG CATTGGAGTCTGTGC-3'; GAPDH forward, 5'-TGTTGCCAT CAATGACCCCTT-3', and reverse, 5'-CTCCACGACGTACT CAGCG-3'; U6 forward, 5'-CTCGCTTCGGCAGCACA-3', and reverse, 5'-AACGCTTCACGAATTTGCGT-3'.

### Enzyme-linked immunosorbent assay

Rat hippocampal tissues were mixed with a volume of normal saline 10 times the tissue mass. Then, hippocampal tissues were homogenized in a Bioprep-24 tissue homogenizer (Allsheng, Hangzhou, Zhejiang, China) and centrifuged (4000 rpm) to collect the supernatants. The levels of the brain biomarkers brain-derived neurotrophic factor (BDNF), monocyte chemoattractant protein-1 (MCP-1), and homocysteine (Hcy) were measured in the supernatant samples or cell supernatants according to the manufacturer's instructions. All results were obtained by measuring the optical density using a microplate reader. The BDNF (cat. no. EK0308) ELISA kit was purchased from Boster Bioengineering Company (Wuhan, China). The MCP-1 (cat. no. SBJ-R0616) and Hcy (cat. no. SBJ-R0319) ELISA kits were purchased from SenBeijia Biological Technology (Nanjing, China).

### Flow cytometry analysis

Flow cytometry analysis was performed to assess neuronal apoptosis. Using an Annexin V/FITC kit (Neo Bioscience, Beijing, China), apoptotic cells were double-labeled with Annexin V-fluorescein isothiocyanate and propidium iodide. Then, a BDTM LSRII flow cytometer (BD Biosciences, Franklin Lakes, NJ, USA) was used to analyze the cells. In the flow cytometry output, cells in the 3rd quadrant (Q3) represented apoptotic cells.

### Morris water maze

Seven weeks after 2VO surgery, the Morris water maze was used to evaluate spatial learning and memory.<sup>12</sup> Briefly, the maze consisted of a 2.0-m-diameter circular tank (with opaque water at a temperature of 25±1°C), and was conceptually separated into four quadrants. The pool was surrounded with black curtains to block extramaze cues. A small white platform (20 cm in diameter, 20 cm in height) was submerged 2 cm below the water surface, and the water was dyed with black food pigment. The rats were trained to search for the escape platform from a distal starting location in the center of the first quadrant. For cued training (three trials/day for 5 consecutive days), the rats were put into the water facing the sidewall. The rats were permitted to rest on the platform for 20 s. The time it took for the rat to discover the platform was defined as the escape latency. On day 5, the platform was removed after the last trial. On day 6, the probe trial was performed. The rats were allowed to swim for 120 s. The online DigBehav-Morris Water Maze Video Analysis System (Mobile Datum Software Technology

Co., Ltd., Shanghai, China) was used to monitor the escape latency (s) and number of platform crosses.

### Western blot analysis

Radioimmunoprecipitation assay buffer (cat. no. 9800; Cell Signaling Technology, Inc., 3 Trask Lane Danvers, Boston, MA, USA) was used to lyse NRNs to obtain protein. Then, the concentration of protein was determined with the bicinchoninic acid protein quantitative kit (cat. no. P0010S; Beyotime, Shanghai, China). The proteins were separated by 10% sodium dodecyl sulfate polyacrylamide gel electrophoresis and then transferred to polyvinylidene difluoride membranes (cat. no. IPVH00010; Millipore, Billerica, MA, USA). After blocking with 5% skimmed milk, the membranes were incubated with TSPAN5 (cat. no. ab236881; Abcam, Cambridge, UK) and GAPDH (cat. no. ab9485; Abcam) antibodies overnight at 4°C. Subsequently, the membranes were incubated with a horse-

radish peroxidase-conjugated anti-rabbit IgG secondary antibody (cat. no. 7074; Cell Signaling Technology, Inc.) at room temperature for 2 h. Eventually, an enhanced electrochemiluminescence detection system (Millipore) was applied to visualize the bands.

### Bioinformatics analysis

The online database starBase (<http://starbase.sysu.edu.cn/>) was used to predict the downstream targets that have binding sites for miR-322-5p (search category: microT, miRanda, miRmap, PITA, RNA22, PicTar, and TargetScan). The binding site of rno-miR-322-5p in TSPAN5 was predicted in TargetScan database ([http://www.targetscan.org/vert\\_70/](http://www.targetscan.org/vert_70/)).

### Dual-luciferase reporter gene assay

The dual-luciferase reporter assay was used to assess binding affinity between miR-322-5p and TSPAN5. The 3'-UTR of

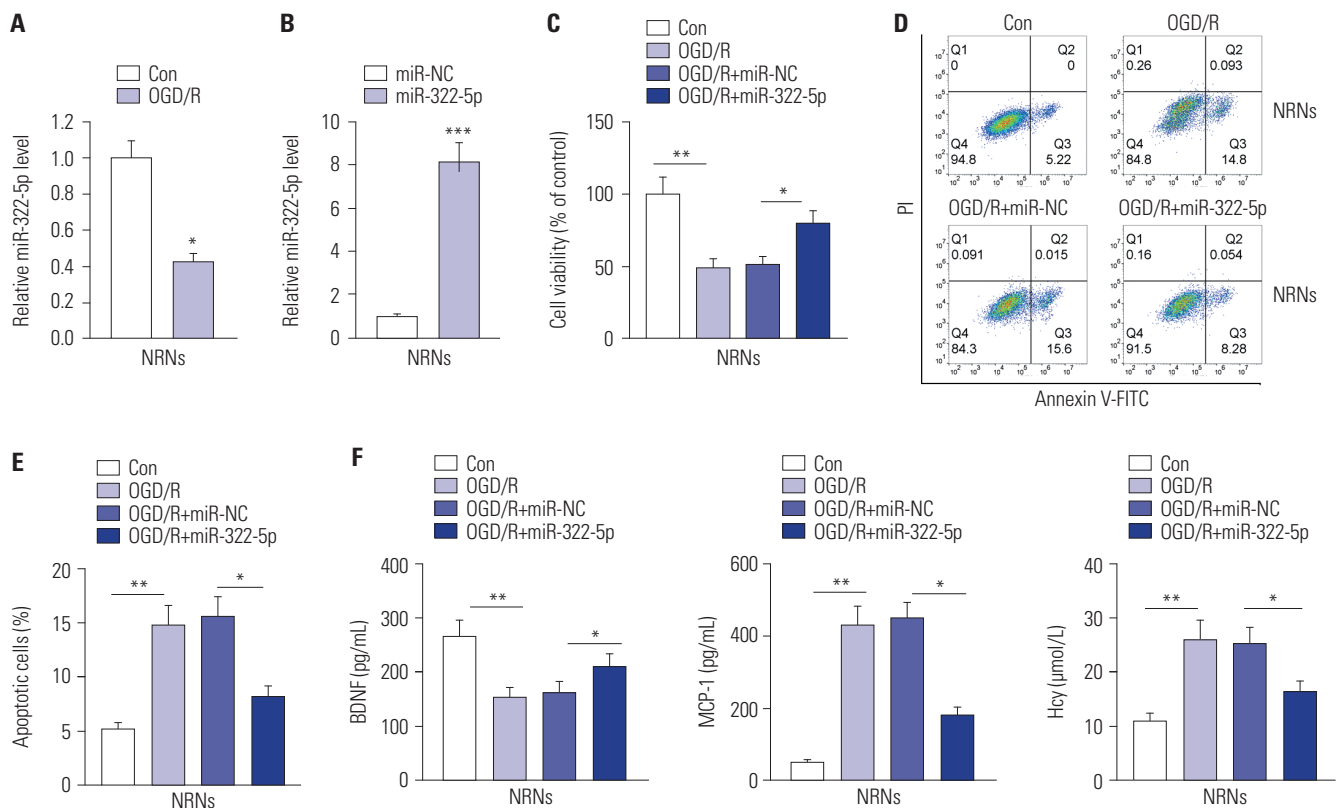


**Fig. 1.** MiR-322-5p overexpression inhibits neuronal injury. (A) RT-qPCR analysis was used to assess the miR-322-5p level in OGD/R-treated NRNs and control NRNs. Quantification of miR-322-5p expression showed a 2.5-fold decrease in OGD/R-treated NRNs compared to controls. \* $p < 0.05$ , Student's t-test. (B) The miR-322-5p level in OGD/R-treated NRNs transfected with miR-NC or miR-322-5p was measured by RT-qPCR. The miR-322-5p level was significantly upregulated after miR-322-5p transfection. \*\*\* $p < 0.001$ , Student's t-test. (C) Neuronal viability was evaluated by the MTT assay in OGD/R-treated NRNs transfected with miR-NC or miR-322-5p. Overexpression of miR-322-5p increased the viability of OGD/R-treated NRNs. \* $p < 0.05$ , \*\* $p < 0.01$ , ANOVA followed by Tukey's post hoc test. (D and E) Apoptotic cells in OGD/R-treated NRNs transfected with miR-NC or miR-322-5p were analyzed by flow cytometry. Overexpression of miR-322-5p reduced the apoptosis of OGD/R-treated NRNs. \* $p < 0.05$ , \*\* $p < 0.01$ , ANOVA followed by Tukey's post hoc test. (F) The levels of BDNF, MCP-1, and Hcy in neuronal supernatants from the indicated groups were examined by ELISA. Overexpression of miR-322-5p increased BDNF expression and reduced MCP-1 and Hcy expression in OGD/R-treated NRNs. \* $p < 0.05$ , \*\* $p < 0.01$ , ANOVA followed by Tukey's post hoc test. The data are presented as the means  $\pm$  SD. RT-qPCR, reverse transcription-quantitative PCR; OGD/R, oxygen-glucose deprivation/reoxygenation; NRNs, neonatal rat neurons; MTT, 3-(4,5-Dimethylthiazol-2-yl)-2,5-diphenyltetrazolium bromide; NC, negative control; ANOVA, analysis of variance; BDNF, brain-derived neurotrophic factor; MCP-1, monocyte chemoattractant protein-1; Hcy, homocysteine; ELISA, enzyme-linked immunosorbent assay.

TSPAN5 was inserted into the pmirGLO reporter vector (cat. no. E1330; Promega, Madison, WI, USA) to construct a wild-type TSPAN5-expressing vector.<sup>19</sup> Site specific mutagenesis of TSPAN5 was performed to generate mutant (Mut) TSPAN5. MiR-322-5p mimics (or NC mimics) were co-transfected with these plasmids into NRNs using Lipofectamine 2000. After 48 h, luciferase activity was assessed through a Dual-Luciferase Reporter System (Promega).

**Statistical analysis**

Data are presented as the mean±SD and were analyzed using SPSS 20.0 (IBM Corp., Armonk, NY, USA). Each experiment was repeated three times. Student’s t-test or one-way analysis of variance (ANOVA) followed by Tukey’s post hoc test was

used for comparisons between groups. The correlation between miR-322-5p expression and TSPAN5 expression was analyzed by Pearson Correlation analysis. A  $p < 0.05$  was considered statistically significant.

**RESULTS**

**MiR-322-5p overexpression inhibits neuronal injury**

Previously, miR-322-5p was found to have a downregulated expression and exert a neuroprotective effect in neurodegenerative diseases.<sup>16,20</sup> Therefore, in this study, we aimed to explore the role of miR-322-5p in NRNs. As shown in Fig. 1A, quantification of miR-322-5p expression showed a 2.5-fold de-

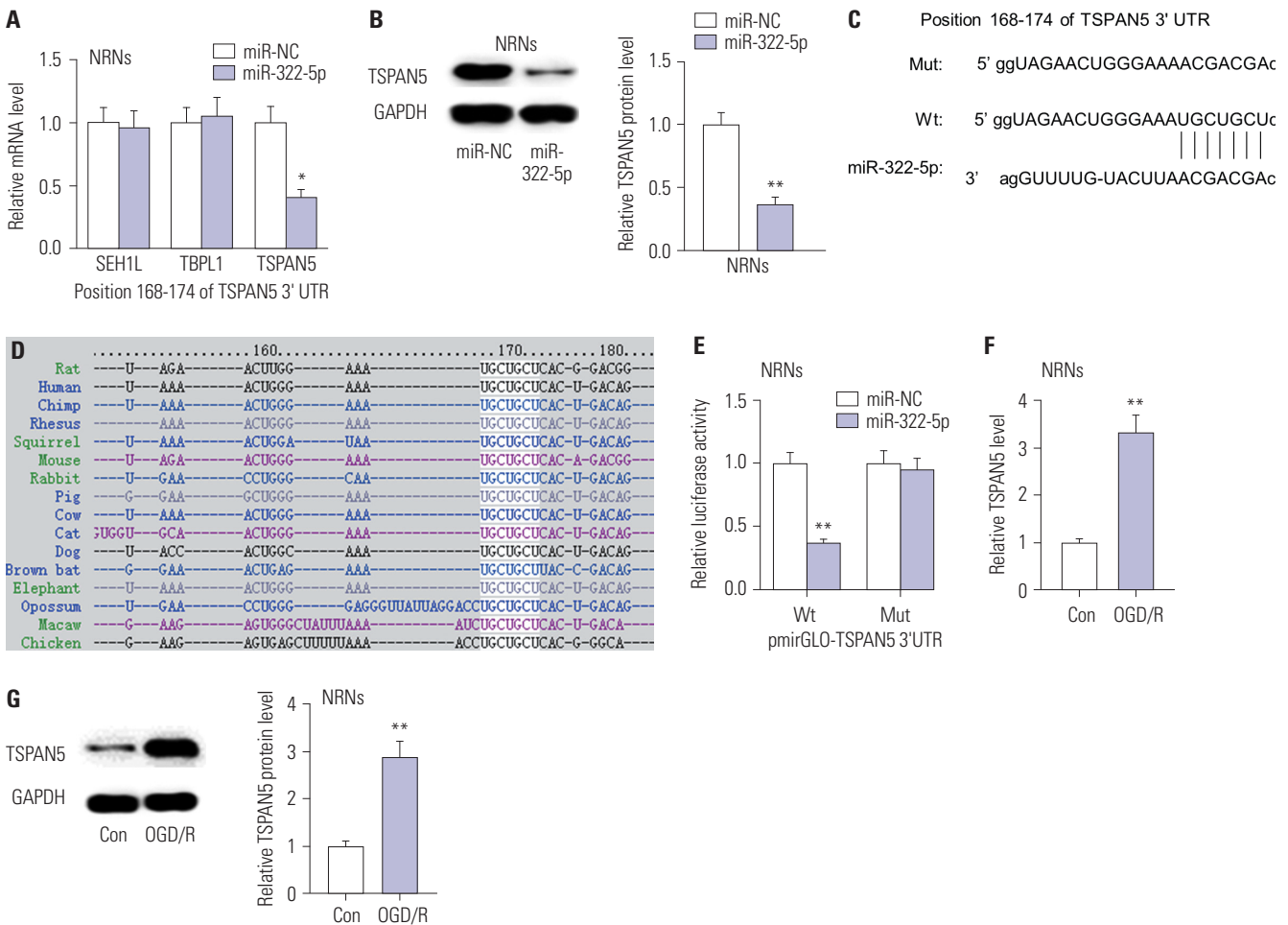


**Fig. 2.** MiR-322-5p directly targets TSPAN5. (A) The mRNA levels of SEH1L, TBPL1, and TSPAN5 in NRNs transfected with miR-NC or miR-322-5p were determined by RT-qPCR analysis. Overexpression of miR-322-5p significantly reduced TSPAN5 mRNA expression. \* $p < 0.05$ , ANOVA followed by Tukey’s post hoc test. (B) The TSPAN5 protein level in NRNs transfected with miR-NC or miR-322-5p was determined by western blot. Overexpression of miR-322-5p significantly reduced TSPAN5 protein expression. \*\* $p < 0.01$ , Student’s t-test. (C and D) The binding site of miR-322-5p in TSPAN5 was predicted at the TargetScan website. (E) The binding ability of miR-322-5p to TSPAN5 was confirmed through a luciferase reporter assay. Overexpression of miR-322-5p reduced luciferase activity of the pmirGLO-TSPAN5 3’-UTR-Wt vector compared to that of the pmirGLO-TSPAN5 3’-UTR-Mut vector. \*\* $p < 0.01$ , ANOVA followed by Tukey’s post hoc test. (F and G) The TSPAN5 mRNA and protein levels in OGD/R-treated NRNs and control NRNs were measured by RT-qPCR and western blot. OGD/R significantly upregulated the TSPAN5 mRNA and protein levels. The graphs represent the average value of the band intensity for each blot, and each blot was normalized to the band intensity value of GAPDH. \*\* $p < 0.01$ , Student’s t-test. The data are presented as the means±SD. TSPAN5, tetraspanin 5; NRNs, neonatal rat neurons; NC, negative control; RT-qPCR, reverse transcription-quantitative PCR; ANOVA, analysis of variance; OGD/R, oxygen-glucose deprivation/reoxygenation.

crease in OGD/R-treated NRNs compared to controls ( $p < 0.05$ , Student's *t*-test). Additionally, miR-322-5p expression was up-regulated after miR-322-5p transfection in OGD/R-treated NRNs ( $p < 0.001$ , Student's *t*-test) (Fig. 1B). According to the MTT assay, the viability of OGD/R-treated NRNs was reduced more than 2-fold compared to that of controls ( $p < 0.01$ , ANOVA followed by Tukey's post hoc test), while miR-322-5p overexpression reversed the suppressive effects of OGD/R on cell viability ( $p < 0.05$ , ANOVA followed by Tukey's post hoc test) (Fig. 1C). Furthermore, the increase in the number of apoptotic cells resulting from OGD/R treatment was counteracted by miR-322-5p overexpression ( $p < 0.05$ , ANOVA followed by Tukey's post hoc test) (Fig. 1D and E). Finally, OGD/R induced a reduction in BDNF expression and an increase in MCP-1 and Hcy expression ( $p < 0.01$ , ANOVA followed by Tukey's post hoc test), which was reversed by miR-322-5p overexpression ( $p < 0.05$ , ANOVA followed by Tukey's post hoc test) (Fig. 1F). In summary, the OGD/R-induced cell injury is alleviated by miR-322-5p overexpression.

### MiR-322-5p directly targets TSPAN5

A multitude of studies have shown that miR-322-5p can inhibit the translation of mRNA(s) by binding to the 3'-UTRs of mRNAs.<sup>14,21,22</sup> With the assistance of starBase (<http://starbase.sysu.edu.cn/>), three mRNAs (SEH1L, TBPL1, and TSPAN5) were predicted to have binding sites for miR-322-5p. Additionally, in cells with miR-322-5p overexpression, TSPAN5 expression was significantly downregulated ( $>2$ -fold) ( $p < 0.05$ , ANOVA followed by Tukey's post hoc test), while SEH1L and TBPL1 expression displayed no significant change (Fig. 2A). Moreover, TSPAN5 protein expression showed a 2.6-fold decrease in miR-322-5p-transfected NRNs compared to controls ( $p < 0.01$ , Student's *t*-test) (Fig. 2B). According to the TargetScan database ([http://www.targetscan.org/vert\\_70/](http://www.targetscan.org/vert_70/)), the binding site of miR-322-5p at position 168-174 of TSPAN5 3'-UTR is presented in Fig. 2C. Their binding site is highly conserved in multiple species (Fig. 2D). Through a luciferase reporter assay, a reduced luciferase activity of the pmirGLO-TSPAN5 3'-UTR-Wt vector was observed in the miR-322-5p overexpression group ( $p < 0.01$ , ANOVA followed by Tukey's post hoc test), but no significant change in the luciferase activity of the pmirGLO-

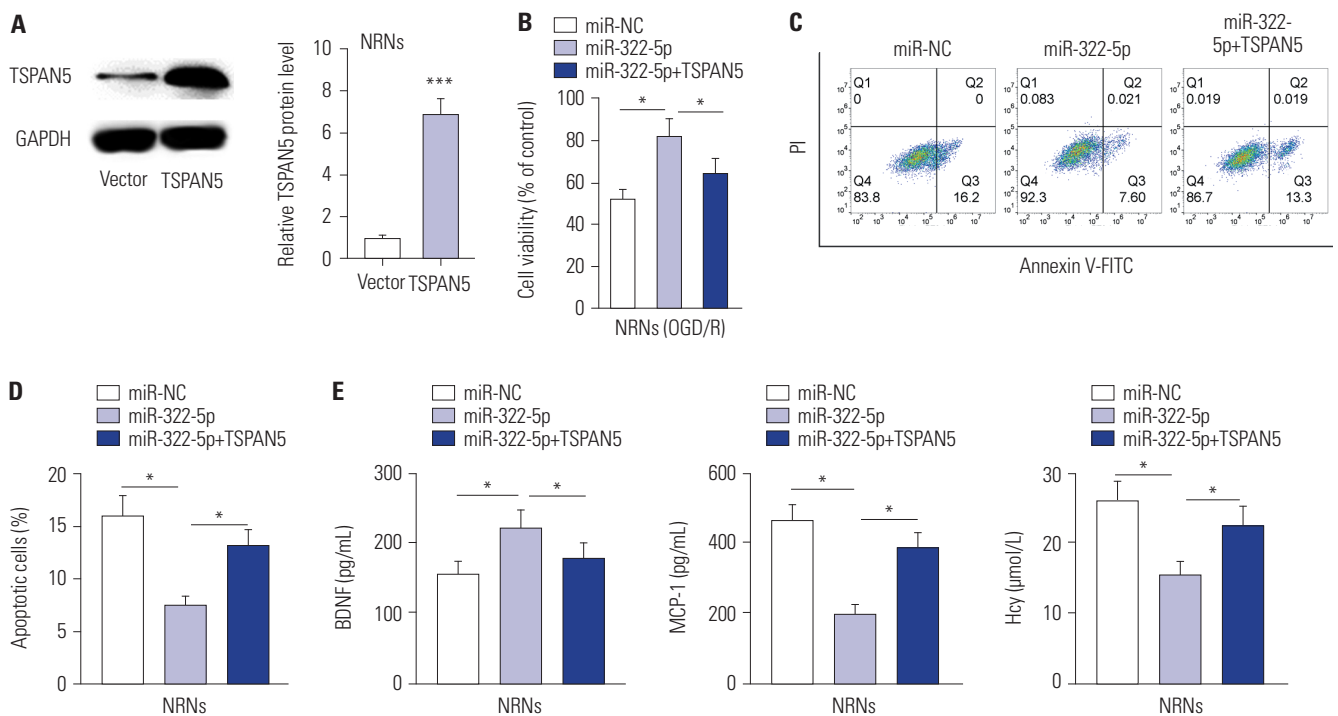


**Fig. 3.** MiR-322-5p regulates OGD/R-induced neuronal injury by regulating TSPAN5. (A) The overexpression efficiency of pcDNA3.1/TSPAN5 in NRNs was verified by western blot. TSPAN5 protein expression was increased more than 6-fold after transfection with pcDNA3.1/TSPAN5. \*\*\* $p < 0.001$ , Student's *t*-test. (B) Neuronal viability in OGD/R-treated NRNs transfected with the indicated plasmids was evaluated by the MTT assay. The increase in cell viability resulting from miR-322-5p overexpression was counteracted by TSPAN5 overexpression. \* $p < 0.05$ , ANOVA followed by Tukey's post hoc test. (C and D) Apoptotic cells in OGD/R-treated NRNs transfected with the indicated plasmids were evaluated by flow cytometry. The inhibitory influence of miR-322-5p on apoptotic neurons was reversed by TSPAN5 overexpression. \* $p < 0.05$ , ANOVA followed by Tukey's post hoc test. (E) The concentrations of BDNF, MCP-1, and Hcy in OGD/R-treated NRNs transfected with the indicated plasmids were assessed by ELISA. The miR-322-5p-mediated increase in BDNF expression and decrease in MCP-1 and Hcy expression were reversed by TSPAN5 overexpression. \* $p < 0.05$ , ANOVA followed by Tukey's post hoc test. The data are presented as the means  $\pm$  SD. TSPAN5, tetraspanin 5; NRNs, neonatal rat neurons; RT-qPCR, reverse transcription-quantitative PCR; ANOVA, analysis of variance; OGD/R, oxygen-glucose deprivation/reoxygenation; BDNF, brain-derived neurotrophic factor; MCP-1, monocyte chemoattractant protein-1; Hcy, homocysteine.

TSPAN5 3'-UTR-Mut vector was observed (Fig. 2E). Moreover, TSPAN5 mRNA and protein expression was upregulated in OGD/R-treated NRNs ( $p < 0.01$ , Student's t-test) (Fig. 2F and G). Overall, TSPAN5 is a target of miR-322-5p.

**MiR-322-5p regulates OGD/R-induced neuronal injury by targeting TSPAN5**

To validate whether miR-322-5p influences cell injury by regulating TSPAN5, rescue assays were performed in OGD/R-treated NRNs. First, TSPAN5 protein expression was increased more than 6-fold after transfection with pcDNA3.1/TSPAN5 ( $p < 0.01$ , Student's t-test) (Fig. 3A). Moreover, the increase in cell viability resulting from miR-322-5p overexpression was counteracted by TSPAN5 overexpression ( $p < 0.05$ , ANOVA followed by Tukey's post hoc test) (Fig. 3B). Additionally, the inhibitory influence of miR-322-5p overexpression on apoptotic neurons was reversed by TSPAN5 overexpression ( $p < 0.05$ , ANOVA followed by Tukey's post hoc test) (Fig. 3C and D). Finally, the miR-322-5p overexpression-mediated increase in BDNF expression and decrease in MCP-1 and Hcy expression were reversed by TSPAN5 overexpression ( $p < 0.05$ , ANOVA followed by Tukey's post hoc test) (Fig. 3E). In summary, miR-322-5p regulates OGD/R-induced neuronal injury by regulating TSPAN5.

**MiR-322-5p alleviates impairment of cognitive function in rats**

We then explored the role of miR-322-5p in vivo. As shown in Fig. 4A, the miR-322-5p level was decreased nearly 2-fold in the hippocampi of 2VO rats compared to those of sham rats ( $p < 0.05$ , ANOVA followed by Tukey's post hoc test), and miR-322-5p was significantly overexpressed after injection of LV-miR-322-5p ( $p < 0.01$ , ANOVA followed by Tukey's post hoc test). Furthermore, miR-322-5p overexpression shortened the latency to reach the platform in 2VO rats ( $p < 0.05$ , ANOVA followed by Tukey's post hoc test) (Fig. 4B). Moreover, the mice in the 2VO+LV-miR-322-5p group crossed the platform more times than those in the 2VO+LV-NC group ( $p < 0.05$ , ANOVA followed by Tukey's post hoc test) (Fig. 4C). According to RT-qPCR, the TSPAN5 level was decreased more than 2-fold after injection of LV-miR-322-5p in the hippocampi ( $p < 0.05$ , ANOVA followed by Tukey's post hoc test) (Fig. 4D). Finally, the TSPAN5 level was negatively correlated with the miR-322-5p level in the hippocampi (Fig. 4E). These data showed that miR-322-5p mitigates cognitive dysfunction in 2VO rats.

**Effect of miR-322-5p and TSPAN5 on the expression of important biomarkers**

We next assessed the levels of BDNF, MCP-1, and Hcy in each

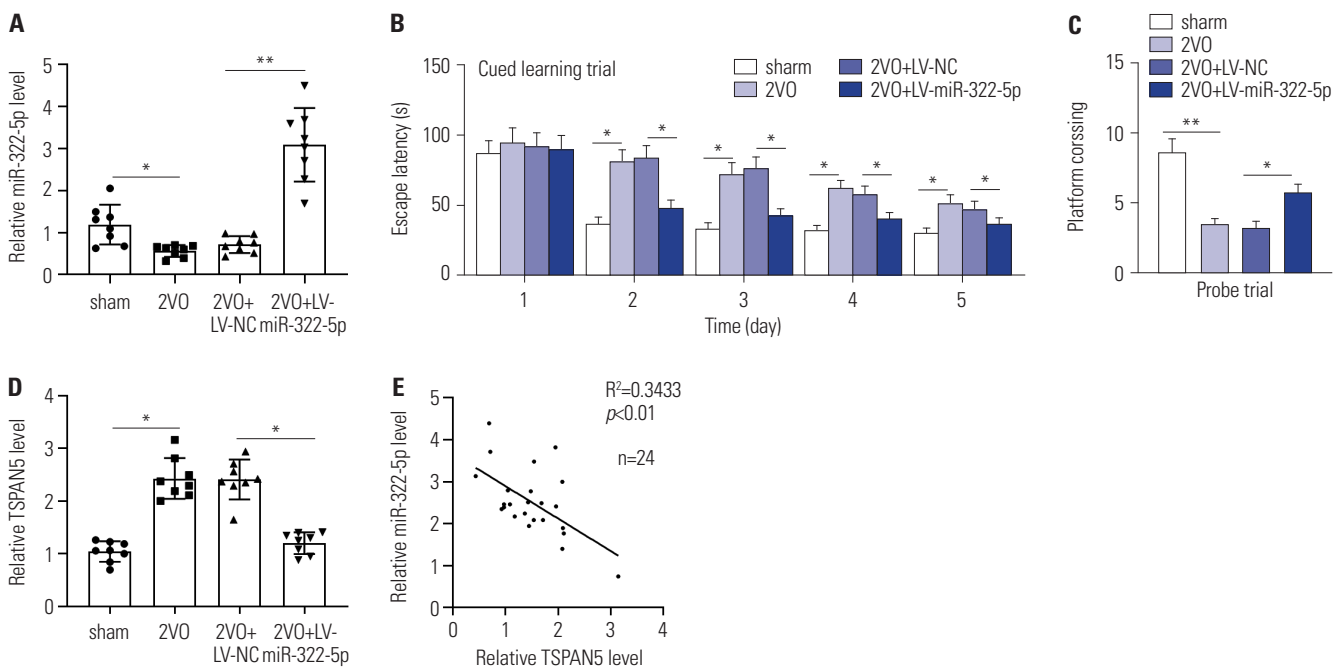


**Fig. 4.** MiR-322-5p alleviates the impairment of cognitive function in rats. (A) The overexpression efficiency of LV-miR-322-5p in the hippocampus was verified by RT-qPCR. The level of miR-322-5p was significantly increased after injection of LV-miR-322-5p. \* $p < 0.05$ , \*\* $p < 0.01$ , ANOVA followed by Tukey's post hoc test. (B) The average latency to find the platform was determined for different groups ( $n = 8$ /group). Overexpression of miR-322-5p shortened the latency to reach the platform in 2VO rats. \* $p < 0.05$ , ANOVA followed by Tukey's post hoc test. (C) The number of platform crossings was measured for different groups ( $n = 8$ /group). The mice in the 2VO+LV-miR-322-5p group crossed the platform more times than did those in the 2VO+LV-NC group. \* $p < 0.05$ , \*\* $p < 0.01$ , ANOVA followed by Tukey's post hoc test. (D) The TSPAN5 level in the rat hippocampi was verified by RT-qPCR in different groups ( $n = 8$ /group). The TSPAN5 level was decreased more than 2-fold by LV-miR-322-5p in the hippocampi. \* $p < 0.05$ , ANOVA followed by Tukey's post hoc test. (E) The correlation between miR-322-5p expression and TSPAN5 expression in the hippocampi was analyzed by Pearson Correlation analysis. The TSPAN5 level was negatively correlated with the miR-322-5p level in the hippocampi. The data are presented as the means  $\pm$  SD. LV, lentiviral vector; RT-qPCR, reverse transcription-quantitative PCR; ANOVA, analysis of variance; TSPAN5, tetraspanin 5.

group *in vivo*. The ELISA results showed that the 2VO group had significantly reduced levels of BDNF and increased levels of MCP-1 and Hcy ( $p < 0.01$ , ANOVA followed by Tukey's post hoc test), while injection of LV-miR-322-5p reversed these changes ( $p < 0.05$ , ANOVA followed by Tukey's post hoc test) (Fig. 5A-C), further suggesting the role of miR-322-5p in alleviating cognitive dysfunction. Furthermore, TSPANS expression regulation alone was determined. As shown in Fig. 5D-F, the injection of LV-sh-TSPANS significantly increased the levels of BDNF and reduced the levels of MCP-1 ( $p < 0.01$ , ANOVA followed by Tukey's post hoc test) and Hcy ( $p < 0.05$ , ANOVA followed by Tukey's post hoc test) in 2VO rats. This suggested that knockdown of TSPANS alleviates cognitive dysfunction.

## DISCUSSION

The roles of miRNAs in the pathogenesis of vascular dementia have been widely studied, and further investigations of therapies that target miRNAs are considered important.<sup>23,24</sup> The results of the present study indicated that miR-322-5p was associated with the development of vascular dementia. As previously

reported, miR-322 treatment rescues cell apoptosis and neural tube defect formation through silencing NADPH oxidase 4.<sup>25</sup> Hippocampal neuron death is a key factor in vascular dementia induced by CBH.<sup>26</sup> Multiple studies used the OGD/R *in vitro* model in neurons for the investigation of vascular dementia.<sup>26-28</sup> In our study, miR-322-5p showed a significantly low expression in OGD/R-treated NRNs. We then upregulated the expression of miR-322-5p and found that OGD/R-induced cell injury was alleviated by miR-322-5p overexpression. CBH is considered a preclinical condition of mild cognitive impairment and is thought to precede dementia. Permanent bilateral common carotid artery occlusion (2VO) is a well-characterized method for investigating cognitive functions and histopathological consequences of CBH in rats.<sup>29</sup> According to previous studies,<sup>30,31</sup> 2VO surgery is a classic animal model for investigating pathological process of vascular dementia. In our work, 2VO induced significant brain injury and impaired learning ability in rats. Moreover, overexpression of miR-322-5p ameliorated neuronal injury *in vitro* and alleviated the impairment of cognitive function in rats. Therefore, our study showed that miR-322-5p may be a target for vascular dementia. However, the reduction in miR-322-5p expression in the models we observed differs from

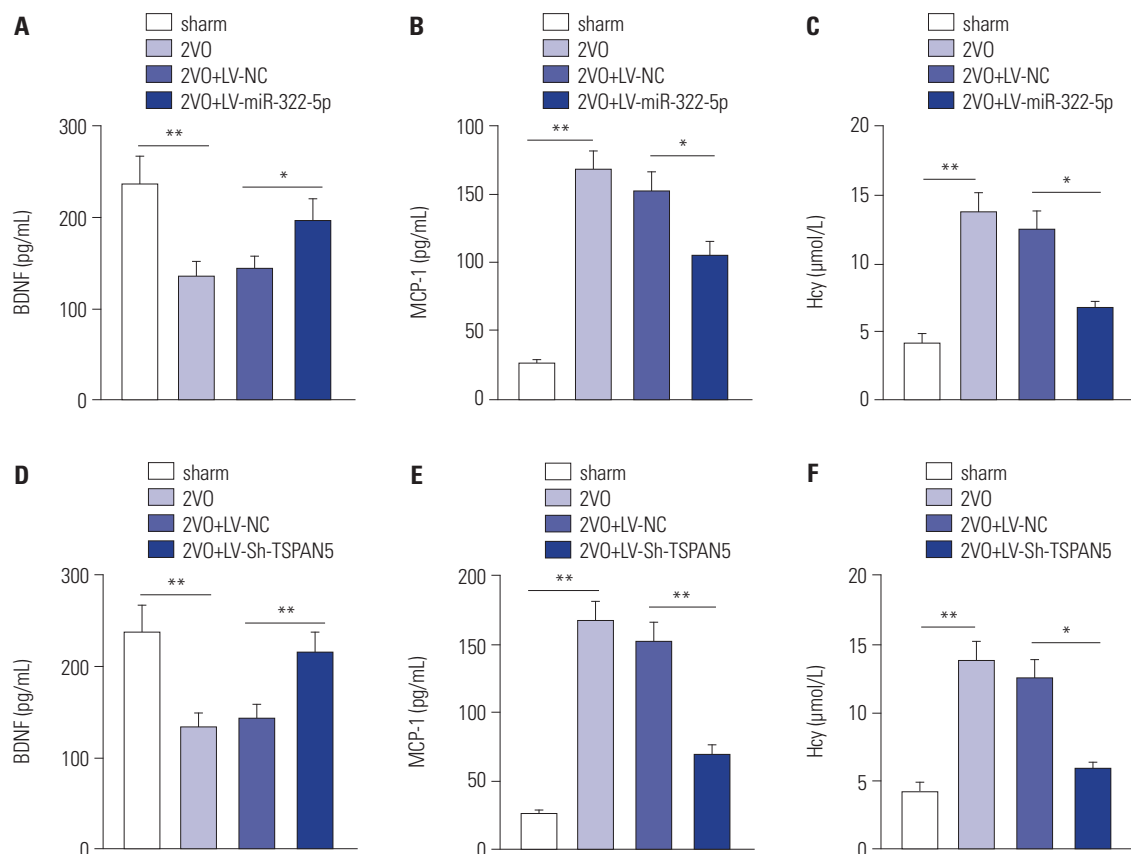


**Fig. 5.** Effect of miR-322-5p and TSPAN5 on the expression of important biomarkers. (A-F) The concentrations of BDNF, MCP-1, and Hcy were assessed by ELISA in the hippocampi of rats from different groups ( $n=8/\text{group}$ ). Injection of LV-miR-322-5p or LV-sh-TSPANS significantly increased the levels of BDNF and reduced the levels of MCP-1 in 2VO rats. \* $p < 0.05$ , \*\* $p < 0.01$ , ANOVA followed by Tukey's post hoc test. The data are presented as the means  $\pm$  SD. BDNF, brain-derived neurotrophic factor; MCP-1, monocyte chemoattractant protein-1; Hcy, homocysteine; ELISA, enzyme-linked immunosorbent assay.



previously reported changes in miR-322-5p expression in Alzheimer's disease.<sup>16</sup> It is highly suggestive of the tissue specificity of miR-322-5p, depending on the cellular and molecular context.

MicroRNAs can directly target the 3'-UTRs of corresponding mRNAs to control gene expression posttranscriptionally.<sup>32-34</sup> Moreover, miR-322-5p can also inhibit the translation of mRNA(s) by targeting the 3'-UTRs of mRNAs.<sup>14,21,22</sup> Bioinformatics analysis was performed to identify the targets of miR-322-5p. We further confirmed that TSPAN5 was directly targeted and negatively regulated by miR-322-5p. The TSPAN5 protein, also known as TM4SF9, is a member of the transmembrane 4 superfamily or tetraspanin family.<sup>35</sup> Most members of this family are located on the cell surface and contain four hydrophobic domains.<sup>36,37</sup> A multitude of studies have reported that these proteins mediate signal transduction and then exert effects on cell growth, activation, and motility.<sup>38-41</sup> In detail, tetraspanin 3 (Tspan3) was identified to be upregulated in the brains of Alzheimer's disease patients and to activate A Disintegrin and Metalloproteinase 10 (ADAM10), APP, and the  $\gamma$ -secretase complex in the context of Alzheimer's disease.<sup>42</sup> Moreover, TSPAN5 was also shown to promote Notch activity by affecting the ADAM10 levels and acting at the gamma-secretase cleavage step.<sup>38,43</sup> In the current study, we found that TSPAN5 had a high expression level in OGD/R-treated NRNs and the hippocampi of 2VO rats. Through rescue assays, we also found that overexpression of TSPAN5 countered the effects of miR-322-5p overexpression on neuronal injury. More importantly, the *in vivo* experiments showed that the knockdown of TSPAN5 alleviated cognitive dysfunction in 2VO rats.

In summary, this study is the first to demonstrate that miR-322-5p alleviated cell injury and impaired cognitive function in the context of vascular dementia by targeting TSPAN5. The miR-322-5p/TSPAN5 axis may be a potential regulatory mechanism for investigating cognitive function. This study may provide important findings for the clinical diagnosis and treatment of dementia in the future. Nevertheless, our study has some limitations. First, the detailed mechanisms by which OGD/R treatment or 2VO mediates dysregulation of miR-322-5p and TSPAN5 remain unclear. Second, other regulatory mechanisms of miR-322-5p in the context of vascular dementia deserve further exploration. Additionally, more experimental models with clinical significance should be developed to support our conclusions.

## ACKNOWLEDGEMENTS

This work was supported by a grant from the Training Program for Scientific Research of The Affiliated Lianyungang Oriental Hospital of Xuzhou Medical University (No. KY2018006).

## AUTHOR CONTRIBUTIONS

**Conceptualization:** all authors. **Data curation:** Wei Zheng, Bin Zhou, and Huanxian Chang. **Formal analysis:** Jie Zhang and Bin Zhou. **Funding acquisition:** Wei Zheng and Jie Zhang. **Investigation:** Wei Zheng and Jie Zhang. **Methodology:** Wei Zheng. **Project administration:** Jie Zhang. **Resources:** Bin Zhou and Huanxian Chang. **Software:** Bin Zhou and Huanxian Chang. **Supervision:** Jie Zhang. **Validation:** Wei Zheng, Bin Zhou, and Huanxian Chang. **Visualization:** Wei Zheng. **Writing—original draft:** Wei Zheng. **Writing—review & editing:** Wei Zheng and Jie Zhang. **Approval of final manuscript:** all authors.

## ORCID iDs

Wei Zheng	<a href="https://orcid.org/0000-0001-7193-1185">https://orcid.org/0000-0001-7193-1185</a>
Jie Zhang	<a href="https://orcid.org/0000-0002-7117-4396">https://orcid.org/0000-0002-7117-4396</a>
Bin Zhou	<a href="https://orcid.org/0000-0002-6080-3230">https://orcid.org/0000-0002-6080-3230</a>
Huanxian Chang	<a href="https://orcid.org/0000-0003-0698-6694">https://orcid.org/0000-0003-0698-6694</a>

## REFERENCES

1. Ueno M, Chiba Y, Matsumoto K, Murakami R, Fujihara R, Kawachi M, et al. Blood-brain barrier damage in vascular dementia. *Neuropathology* 2016;36:115-24.
2. Di Marco LY, Venneri A, Farkas E, Evans PC, Marzo A, Frangi AF. Vascular dysfunction in the pathogenesis of Alzheimer's disease--A review of endothelium-mediated mechanisms and ensuing vicious circles. *Neurobiol Dis* 2015;82:593-606.
3. Jing Z, Shi C, Zhu L, Xiang Y, Chen P, Xiong Z, et al. Chronic cerebral hypoperfusion induces vascular plasticity and hemodynamics but also neuronal degeneration and cognitive impairment. *J Cereb Blood Flow Metab* 2015;35:1249-59.
4. Schulte C, Karakas M, Zeller T. microRNAs in cardiovascular disease-clinical application. *Clin Chem Lab Med* 2017;55:687-704.
5. Lu TX, Rothenberg ME. MicroRNA. *J Allergy Clin Immunol* 2018; 141:1202-7.
6. Zhang J, Dongwei Z, Zhang Z, Xinhui Q, Kunwang B, Guohui L, et al. miR-let-7a suppresses  $\alpha$ -synuclein-induced microglia inflammation through targeting STAT3 in Parkinson's disease. *Biochem Biophys Res Commun* 2019;519:740-6.
7. Li J, Zhao Y, Choi J, Ting KK, Coleman P, Chen J, et al. Targeting miR-27a/VE-cadherin interactions rescues cerebral cavernous malformations in mice. *PLoS Biol* 2020;18:e3000734.
8. Gámez-Valero A, Guisado-Corcoll A, Herrero-Lorenzo M, Solaguren-Beascoa M, Martí E. Non-coding RNAs as sensors of oxidative stress in neurodegenerative diseases. *Antioxidants (Basel)* 2020;9:1095.
9. Aloizou AM, Siokas V, Sapouni EM, Sita N, Liampas I, Brotis AG, et al. Parkinson's disease and pesticides: are microRNAs the missing link? *Sci Total Environ* 2020;744:140591.
10. Li J, Chen W, Yi Y, Tong Q. miR-219-5p inhibits tau phosphorylation by targeting TTBK1 and GSK-3 $\beta$  in Alzheimer's disease. *J Cell Biochem* 2019;120:9936-46.
11. Ji Y, Wang D, Zhang B, Lu H. MiR-361-3p inhibits  $\beta$ -amyloid accumulation and attenuates cognitive deficits through targeting BACE1 in Alzheimer's disease. *J Integr Neurosci* 2019;18:285-91.
12. Ai J, Sun LH, Che H, Zhang R, Zhang TZ, Wu WC, et al. MicroRNA-195 protects against dementia induced by chronic brain hypoperfusion via its anti-amyloidogenic effect in rats. *J Neurosci* 2013;33:3989-4001.
13. Xie H, Zhao Y, Zhou Y, Liu L, Liu Y, Wang D, et al. MiR-9 regulates

- the expression of BACE1 in dementia induced by chronic brain hypoperfusion in rats. *Cell Physiol Biochem* 2017;42:1213-26.
14. Connolly M, Garfield BE, Crosby A, Morrell NW, Wort SJ, Kemp PR. miR-322-5p targets IGF-1 and is suppressed in the heart of rats with pulmonary hypertension. *FEBS Open Bio* 2018;8:339-48.
  15. Bluhm B, Ehlen HWA, Holzer T, Georgieva VS, Heilig J, Pitzler L, et al. miR-322 stabilizes MEK1 expression to inhibit RAF/MEK/ERK pathway activation in cartilage. *Development* 2017;144:3562-77.
  16. Zhang J, Liu Z, Pei Y, Yang W, Xie C, Long S. MicroRNA-322 cluster promotes tau phosphorylation via targeting brain-derived neurotrophic factor. *Neurochem Res* 2018;43:736-44.
  17. Sun LH, Yan ML, Hu XL, Peng LW, Che H, Bao YN, et al. MicroRNA-9 induces defective trafficking of Nav1.1 and Nav1.2 by targeting Nav $\beta$ 2 protein coding region in rat with chronic brain hypoperfusion. *Mol Neurodegener* 2015;10:36.
  18. Zhao T, Fu Y, Sun H, Liu X. Ligustrazine suppresses neuron apoptosis via the Bax/Bcl-2 and caspase-3 pathway in PC12 cells and in rats with vascular dementia. *IUBMB Life* 2018;70:60-70.
  19. Bränström R, Chang YM, Kasparian N, Affleck P, Tibben A, Aspinwall LG, et al. Melanoma risk factors, perceived threat and intentional tanning: an international online survey. *Eur J Cancer Prev* 2010;19:216-26.
  20. Roshan R, Choudhary A, Bhambri A, Bakshi B, Ghosh T, Pillai B. microRNA dysregulation in polyglutamine toxicity of TATA-box binding protein is mediated through STAT1 in mouse neuronal cells. *J Neuroinflammation* 2017;14:155.
  21. Long Y, Wang L, Li Z. SP1-induced SNHG14 aggravates hypertrophic response in *in vitro* model of cardiac hypertrophy via up-regulation of PCDH17. *J Cell Mol Med* 2020;24:7115-26.
  22. Pang B, Zhen Y, Hu C, Ma Z, Lin S, Yi H. Myeloid-derived suppressor cells shift Th17/Treg ratio and promote systemic lupus erythematosus progression through arginase-1/miR-322-5p/TGF- $\beta$  pathway. *Clin Sci (Lond)* 2020;134:2209-22.
  23. Qian X, Xu Q, Li G, Bu Y, Sun F, Zhang J. Therapeutic effect of idebenone on rats with vascular dementia via the MicroRNA-216a/RSK2/NF- $\kappa$ B axis. *Neuropsychiatr Dis Treat* 2021;17:533-43.
  24. Zhang J, Sun P, Zhou C, Zhang X, Ma F, Xu Y, et al. Regulatory microRNAs and vascular cognitive impairment and dementia. *CNS Neurosci Ther* 2020;26:1207-18.
  25. Liu YS, Gu H, Huang TC, Wei XW, Ma W, Liu D, et al. miR-322 treatment rescues cell apoptosis and neural tube defect formation through silencing NADPH oxidase 4. *CNS Neurosci Ther* 2020;26:902-12.
  26. Li W, Wei D, Lin J, Liang J, Xie X, Song K, et al. Di-3-n-butylphthalide reduces cognitive impairment induced by chronic cerebral hypoperfusion through GDNF/GFR $\alpha$ 1/Ret signaling preventing hippocampal neuron apoptosis. *Front Cell Neurosci* 2019;13:351.
  27. Wang D, Wang Y, Shan M, Chen J, Wang H, Sun B, et al. Apelin receptor homodimer inhibits apoptosis in vascular dementia. *Exp Cell Res* 2021;407:112739.
  28. Zhang Q, Fan Z, Xue W, Sun F, Zhu H, Huang D, et al. Vitexin regulates Epac and NLRP3 and ameliorates chronic cerebral hypoperfusion injury. *Can J Physiol Pharmacol* 2021;99:1079-87.
  29. Song MK, Kim YJ, Lee JM, Kim YJ. Neurovascular integrative effects of long-term environmental enrichment on chronic cerebral hypoperfusion rat model. *Brain Res Bull* 2020;163:160-9.
  30. Ghanbarabadi M, Iranshahi M, Amoueian S, Mehri S, Motamedshariaty VS, Mohajeri SA. Neuroprotective and memory enhancing effects of auraptene in a rat model of vascular dementia: experimental study and histopathological evaluation. *Neurosci Lett* 2016;623:13-21.
  31. Saxena AK, Abdul-Majeed SS, Gurtu S, Mohamed WM. Investigation of redox status in chronic cerebral hypoperfusion-induced neurodegeneration in rats. *Appl Transl Genom* 2015;5:30-2.
  32. Achkar NP, Cambiagno DA, Manavella PA. miRNA biogenesis: a dynamic pathway. *Trends Plant Sci* 2016;21:1034-44.
  33. Mellis D, Caporali A. MicroRNA-based therapeutics in cardiovascular disease: screening and delivery to the target. *Biochem Soc Trans* 2018;46:11-21.
  34. Di Meco A, Praticò D. MicroRNAs as therapeutic targets for Alzheimer's disease. *J Alzheimers Dis* 2016;53:367-72.
  35. Ho MF, Zhang C, Zhang L, Wei L, Zhou Y, Moon I, et al. TSPAN5 influences serotonin and kynurenine: pharmacogenomic mechanisms related to alcohol use disorder and acamprosate treatment response. *Mol Psychiatry* 2021;26:3122-33.
  36. Moretto E, Longatti A, Murru L, Chamma I, Sessa A, Zapata J, et al. TSPAN5 enriched microdomains provide a platform for dendritic spine maturation through neuroligin-1 clustering. *Cell Rep* 2019;29:1130-46.e8.
  37. Kashef J, Diana T, Oelgeschläger M, Nazarenko I. Expression of the tetraspanin family members Tspan3, Tspan4, Tspan5 and Tspan7 during *Xenopus laevis* embryonic development. *Gene Expr Patterns* 2013;13:1-11.
  38. Eschenbrenner E, Jouannet S, Clay D, Chaker J, Boucheix C, Brou C, et al. TspanC8 tetraspanins differentially regulate ADAM10 endocytosis and half-life. *Life Sci Alliance* 2020;3:e201900444.
  39. Matthews AL, Noy PJ, Reyat JS, Tomlinson MG. Regulation of A disintegrin and metalloproteinase (ADAM) family sheddases ADAM10 and ADAM17: the emerging role of tetraspanins and rhomboids. *Platelets* 2017;28:333-41.
  40. Saint-Pol J, Billard M, Dornier E, Eschenbrenner E, Danglot L, Boucheix C, et al. New insights into the tetraspanin Tspan5 using novel monoclonal antibodies. *J Biol Chem* 2017;292:9551-66.
  41. Zhou J, Fujiwara T, Ye S, Li X, Zhao H. Downregulation of Notch modulators, tetraspanin 5 and 10, inhibits osteoclastogenesis *in vitro*. *Calcif Tissue Int* 2014;95:209-17.
  42. Seipold L, Damme M, Prox J, Rabe B, Kasperek P, Sedlacek R, et al. Tetraspanin 3: a central endocytic membrane component regulating the expression of ADAM10, presenilin and the amyloid precursor protein. *Biochim Biophys Acta Mol Cell Res* 2017;1864:217-30.
  43. Dunn CD, Sulis ML, Ferrando AA, Greenwald I. A conserved tetraspanin subfamily promotes Notch signaling in *Caenorhabditis elegans* and in human cells. *Proc Natl Acad Sci U S A* 2010;107:5907-12.